

## Surface Precursor to Magnetic-Domain Nucleation Observed by Secondary-Electron Spin Polarization

R. Allenspach, M. Taborelli, M. Landolt, and H. C. Siegmann

*Laboratorium für Festkörperphysik, Eidgenössische Technische Hochschule, CH-8093 Zürich, Switzerland*  
(Received 18 November 1985)

Nondestructive magnetic depth profiling with spin polarization of secondary electrons reveals a particular magnetic state within the outermost 5 Å of the Fe(100) surface. This state is the first step in reversed-domain nucleation and is best described as a very thin 90° [100] wall, which is forbidden in bulk Fe.

PACS numbers: 79.20.Hx, 75.60.Ch

Anisotropies may keep a ferromagnetic solid in a single-domain state even when the external magnetic field  $H$  is removed. If  $H$  is reversed, a reversed magnetic domain will nucleate prior to coherent rotation of the magnetization  $M$  in most cases. However, the domain-wall energy of the reversed domain establishes a barrier against spontaneous nucleation. Therefore, nucleation centers play a crucial role in the understanding of the coercive force  $H_c$  which is of central importance to technical applications such as magnetic recording. It has frequently been suggested<sup>1</sup> that the surface of a ferromagnet might be a site of reversed-domain nucleation. The specific magnetic behavior at surfaces has successfully been investigated by spin-polarized low-energy electron diffraction.<sup>2-4</sup> Pierce and co-workers<sup>2</sup> observed magnetic hysteresis loops at surfaces with a fixed probing depth characteristic for elastic electron scattering. In this study we utilize the spin polarization of true secondary electrons, which represents a surface magnetometer with the unique property of a tunable probing depth  $z$ , to obtain, in a nondestructive manner, a magnetic depth profile  $M(H, z)$ . This reveals the development of a particular magnetic state of the surface as  $H$  is reversed.

The model system is a single crystal of Fe magnetized along an easy direction [001]. The surface under investigation was chosen to be (100) oriented, which is also an allowed plane of a 180° domain wall. The observed magnetic state is confined to a depth of less than 10 Å from the (100) surface and forms reversibly up to  $H \approx 0.8H_c$ . We show that this state is the first step necessary to build a 180° domain wall and therefore represents a precursor to reversed domain nucleation.

Magnetic hysteresis loops  $M(H)$  have been recorded at various probing depths below the surface by spin polarization measurements of secondary electrons, by the magneto-optic Kerr effect, and by bulk magnetic induction. The experimental setup for the technique employing secondary electrons is the one used earlier<sup>5</sup> for spin-polarized Auger spectroscopy. The sample is magnetized by a small electromagnet with a horse-shoe-shaped iron core providing a magnetic induction

which is, in the range of interest, closely proportional to the applied current (within less than 10%). The absolute value of the applied magnetic field  $H$  cannot be determined accurately in this setup. The Fe(100) surface was prepared by numerous cycles of Ne<sup>+</sup> bombardment at grazing incidence and annealing at 800 K. For the measurement the surface was irradiated with unpolarized primary electrons of variable kinetic energy  $E_p$  between 100 and 2500 eV at 45° off normal, and the emitted electrons were collected at normal emission; the secondary electron kinetic energy  $E_s$  was selected by means of a cylindrical mirror analyzer, and the spin polarization  $P(E_p, E_s, H)$  was measured with a Mott detector. The spin polarization is defined as  $P = (n_{\uparrow} - n_{\downarrow}) / (n_{\uparrow} + n_{\downarrow})$  where  $n_{\uparrow}$  ( $n_{\downarrow}$ ) is the number of electrons with magnetic moment parallel (antiparallel) to  $M$ . The Kerr ellipticity  $\epsilon(H)$  was observed in the transverse mode at a 90° scattering angle by use of a He-Ne laser and a photoelastic modulator allowing for lock-in amplification. Absolute determination of the magnetization  $M$  is not possible from spin polarization  $P$  and Kerr ellipticity  $\epsilon$ . However, we note that for true secondary electrons it has been established<sup>6</sup> that  $P$  is proportional to  $M$ .

The polarization of the secondary electrons provides the magnetic depth profile in the 5–50-Å range by variation of two experimental parameters: the primary-electron kinetic energy  $E_p$ —as was previously described<sup>7</sup>—and, for additional refinement of the depth resolution, the secondary-electron kinetic energy  $E_s$ . Calculated estimates of the depth profiles of secondary-electron emission at various  $E_p$  and  $E_s$  are presented in Fig. 1 for two extreme and one intermediate cases. In the following illustrative description we use a three-step model: hot-electron production, transport to the surface, and emission. The depth distribution of hot-electron production is given by the energy dissipation profile of the primary electrons impinging onto the solid. Inelastic scattering of the hot electrons on their way to the surface then leads to an attenuation which is strongly energy dependent via the energy dependence of the inelastic mean free path (IMFP). The probing depth of secondary electrons

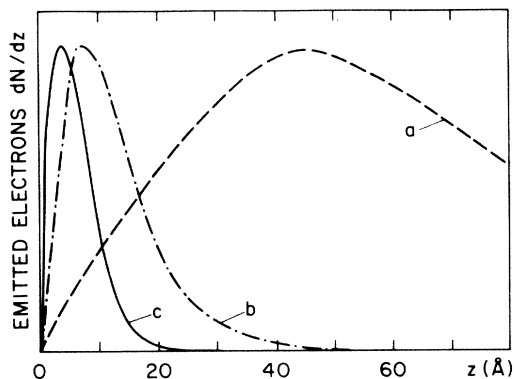


FIG. 1. Calculated profiles  $dN/dz$  of emitted secondary electrons for various primary and secondary electron energies  $E_p$  and  $E_s$ , respectively: *a*,  $E_p = 2500$  eV,  $E_s = 1$  eV; *b*,  $E_p = 200$  eV,  $E_s = 1$  eV; *c*,  $E_p = 200$  eV,  $E_s = 50$  eV.

thus depends on both  $E_p$  and  $E_s$ . We note that the cascade process of hot-electron production includes IMFP effects and makes the division into steps one and two rather artificial. For the estimates of probing depths given in Fig. 1, however, we used calculated energy dissipation profiles for Al from Ganachaud and Cailier,<sup>8</sup> and multiplied them by an exponential attenuation  $I = I_0 \exp[-z/\lambda(E_s)]$ , neglecting multiple scattering during transport to the surface. Here  $\lambda(E_s)$  is the IMFP from the work of Seah and Dench.<sup>9</sup> The lack of a better possibility justifies this simplification, and we expect the result to be qualitatively correct within a factor of 2, since the abundance of hot electrons decreases with increasing kinetic energy. Curve *a* in Fig. 1 represents the case of maximum probing depth of  $z \approx 50$  Å accessible in the present experiment with  $E_p = 2500$  eV and  $E_s = 1$  eV. The remnants of the energy dissipation profile are visible in the line shape, which shows a relatively steep increase at low  $z$  and a large tail towards higher  $z$ . Curve *c* represents a case of extreme surface sensitivity with  $E_p = 200$  eV and  $E_s = 50$  eV, and with *b* we give an intermediate case with  $E_p = 200$  eV and  $E_s = 1$  eV. Figure 1 qualitatively illustrates how the probing depth of secondary electron emission can be varied between  $z \approx 5$  Å and  $z \approx 50$  Å, and that the method even provides depth resolution.

The experimental result is presented in Fig. 2 which shows two magnetic hysteresis loops  $P(H)$  observed with secondary electrons of 1 and 50 eV, respectively, excited with primary electrons of 100 eV at room temperature. These parameters closely correspond to the ones of profiles *b* and *c* in Fig. 1 with probing depths of approximately 10 and 5 Å, respectively.

The hysteresis loop in the upper panel of Fig. 2 recorded with a probing depth of  $\approx 10$  Å is characteristic of a single crystal magnetized along an easy direction. The sharp edges indicate the irreversible motion of a  $180^\circ$  domain wall through the crystal

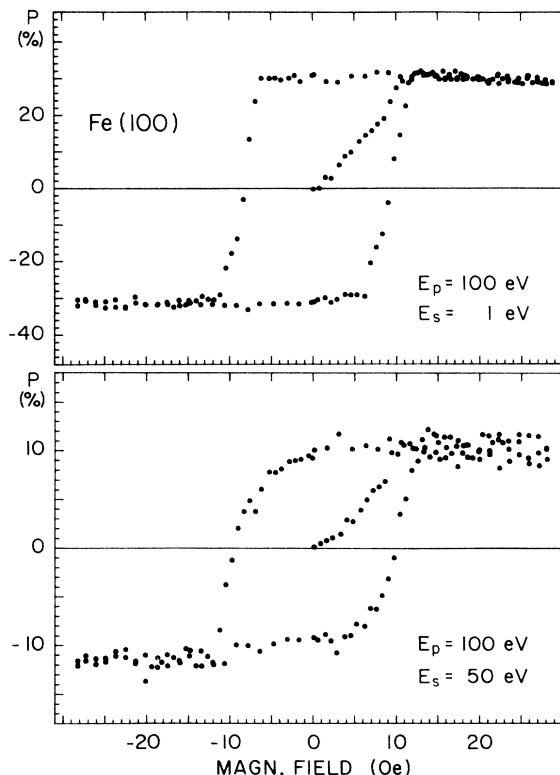


FIG. 2. Magnetic hysteresis loops  $P(H)$  recorded with secondary-electron spin polarization at room temperature. The two curves are obtained with the same primary but different secondary electron energies.

thereby reversing the magnetization to saturation. We note that the hysteresis shows the same behavior when we go deeper into the bulk by raising the primary energy. The spontaneous polarization, however, was found to increase from  $P = 31\%$  at  $E_p = 100$  eV ( $z \approx 10$  Å) to  $P = 46\%$  at  $E_p = 800$  eV ( $z \approx 30$  Å), and to remain constant for higher  $E_p$ . For comparison Fig. 3 shows a bulk hysteresis loop recorded with the Kerr ellipticity  $\epsilon(H)$ , which probes to a depth of  $\approx 200$  Å. The hys-

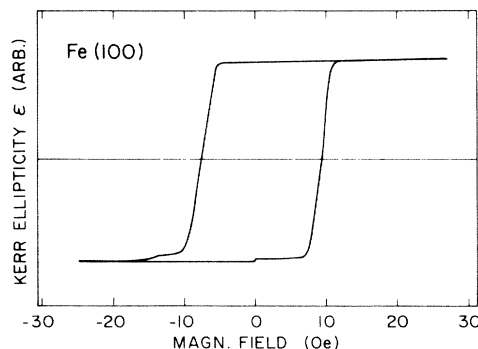


FIG. 3. Magnetic hysteresis loop  $\epsilon(H)$  recorded with Kerr ellipticity.

teresis is the same with the same coercivity.

Only when reducing the probing depth to the outermost 5 Å at the (100) surface by choosing  $E_p = 100$  eV and  $E_s = 50$  eV do we find a drastic change in shape of the hysteresis, as shown in Fig. 2, lower panel. The hysteresis loop is found to be rounded, but still exhibits the same coercivity  $H_c$ .<sup>10</sup>

The magnetic state of the (100) surface of Fe that is uncovered in Fig. 2 has the following features: (1) It appears for  $H$  opposite to the magnetization but less than  $H_c$ . (2) It is reversible in an extended range: For  $H$  opposite to the magnetization and  $|H| \leq 0.8H_c$  removing  $H$  causes  $P$  to return to the value it has had at  $H=0$ . (3) It extends less than 10 Å into the bulk. We emphasize that this depth is considerably smaller than the depth of the thermodynamic reduction of the spontaneous magnetization which reaches as deep as 30 Å at the ambient temperature. (4) The magnetization component  $M(H)$  along [001] steadily decreases to near zero as  $H$  approaches  $-H_c$ .

Our proposal that this magnetic state is a precursor to reversed magnetic-domain nucleation depends on one assumption, namely that there is some organization of the individual spins in the surface sheet. We assume that the magnetization  $M$  in the surface sheet under the influence of the reversed field  $H$  changes its direction but remains unchanged in magnitude, which means that the individual magnetic moments rotate coherently at least within a certain patch along the surface. The exchange interaction between spins in the surface sheet makes the coherent rotation favorable over spin disorder. The measurement by itself only tells that the component along  $H$  decreases. The observation that the magnetization component along [001]  $\rightarrow 0$  for  $H \rightarrow -H_c$  then implies, with the above assumption, that  $M$  is perpendicular to  $H$ . Hence a 90° [100] domain wall is necessary to join the surface magnetization to the bulk which is still magnetized along [001], according to Fig. 2. A 90° [100] wall is forbidden in bulk Fe as it requires additional elastic energy because of magnetostriction. However, the very surface is completely different because of relaxed boundary conditions on the vacuum side and different material properties such as crystalline anisotropy and exchange. This magnetic state of the (100) surface actually is a precursor to reversed-domain nucleation. Under the influence of the reversed magnetic field the magnetization of the outermost  $\approx 5$  Å acquires a *static* state which, at the coercive field  $-H_c$ , fulfills the requirements of a *moving* domain wall. The physical basis of domain-wall motion is the gyroscopic precession of the electron spin, together with damping through spin-lattice relaxation, as described by the Landau-Lifshitz equation.<sup>11</sup> In the present model of the static precursor we have a large component of  $M$  normal to  $H$ . Precession around  $H$  necessarily gen-

erates a nonvanishing component  $M_z$  normal to the surface. The demagnetizing field<sup>11</sup>  $H_z = -4\pi M_z$  then provides the torque to rotate the spins in the subsurface in a (100) plane and hence to form an allowed 180° [100] wall. We note that the critical size of  $H_z$  is determined by strains or defects in the subsurface which is already bulk from the point of view of transition-metal ferromagnetism. The precursor at the surface only provides  $H_z$ , but the critical property leading to  $H_c$  is a subsurface or bulk quality of the sample. This is readily observed by the fact that the Kerr measurements taken in laboratory air show the same coercivity as the clean surface studies under ultrahigh-vacuum conditions.

A last point addresses the handedness of the nascent Bloch wall. The magnetization component  $M_z$  in the surface sheet can assume both signs, inwards or outwards, with equal probability, and the sign of  $M_z$  obviously determines the handedness of the Bloch wall. The surface possibly decomposes into patches of uniform  $M_z$ , and the boundaries between patches of  $M_z$  with opposite signs will generate Bloch lines in the 180° [100] wall to be formed.

The measurement of all three components of the magnetization will further elucidate the particular reversible rotation of  $M$  in the surface sheet. The critical strength  $M_z$  for domain-wall motion can then be determined.

Among the various surface conditions the influence of surface roughness has to be considered in particular. We observe that heavily sputtered surfaces exhibit rounded hysteresis loops even at a depth of 50 Å. Annealing reestablishes the behavior of 180° domain-wall motion with a very shallow precursor state at the surface as depicted in Fig. 2. The role of chemisorption, oxidation of the surface, and the behavior at different crystallographic faces are interesting subjects of future studies.

In conclusion, we state that surface magnetization loops show unexpected differences from bulk, which are revealed only by nondestructive magnetic depth-profiling techniques. We have demonstrated that spin polarization measurements with selected energies of secondary electrons conveniently achieve this goal. The particular magnetic state of a surface at external fields approaching the coercivity readily explains the nucleation of reversed domains at surfaces. Probably, similar processes are active at internal surfaces and interfaces. The concept of the surface precursor of magnetic domain nucleation may prove fruitful in explaining a wealth of material-related observations with potential use in various technologies.

We would like to thank K. Brunner for skillful technical assistance, and we are indebted to F. Heller and M. Haag for performing the bulk magnetization measurements. Financial support by the Nationaler

Energieforschungs-Fonds and the Schweizerischer Nationalfonds is acknowledged.

---

<sup>1</sup>R. Carey and E. D. Isaac, *Magnetic Domains and Techniques for their Observations* (English Universities Press, London, 1966).

<sup>2</sup>R. J. Celotta, D. T. Pierce, G.-C. Wang, S. D. Bader, and G. P. Felcher, Phys. Rev. Lett. **43**, 728 (1979); J. Unguris, D. T. Pierce, and R. J. Celotta, Phys. Rev. B **29**, 1381 (1984).

<sup>3</sup>S. Alvarado, M. Campagna, and H. Hopster, Phys. Rev. Lett. **48**, 51 (1981); D. Weller, S. F. Alvarado, W. Gudat, K. Schröder, and M. Campagna, Phys. Rev. Lett. **54**, 1555 (1985).

<sup>4</sup>G. Waller and U. Gradmann, Phys. Rev. B **26**, 6330 (1982).

<sup>5</sup>M. Landolt and D. Mauri, Phys. Rev. Lett. **49**, 1783 (1982); M. Landolt, R. Allenspach, and D. Mauri, J. Appl. Phys. **57**, 3626 (1985).

<sup>6</sup>J. Glazer, Ph.D. thesis, International School for Advanced Studies, Trieste, 1984 (unpublished).

<sup>7</sup>D. Mauri, R. Allenspach, and M. Landolt, J. Appl. Phys. **58**, 906 (1985).

<sup>8</sup>J. P. Ganachaud and M. Cailler, Surf. Sci. **83**, 519 (1979).

<sup>9</sup>M. P. Seah and W. A. Dench, Surf. Interface Anal. **1**, 1 (1979).

<sup>10</sup>The virgin magnetization curves are also shown in Fig. 2. They exhibit significant  $z$  dependences which will be discussed in a forthcoming publication.

<sup>11</sup>F. H. de Leeuw, R. van den Doel, and U. Enz, Rep. Prog. Phys. **43**, 689 (1980), and references therein.